Turbulent Taylor-Couette Numerical Simulation

Name: Chiao Chun Yang

Home University: University of California, Berkeley

Laboratory: Okano Laboratory

Supervisor: Yasunori Okano

Osaka University Department: Graduate School of Engineering Science

Abstract

Due to the complexity of its flow patterns, turbulent fluid flow has been studied in laboratory experiments as opposed to virtual simulations. However, with the recent advancements in computer technology, it is now possible to numerically model a turbulent system. Furthermore, virtual simulations are oftentimes more financially affordable as opposed to physical experimentation.

My laboratory is interested in reducing the energy loss of large transport ships. Transporting materials across the Pacific Ocean, bulk carrier containers lose more than 60% of its energy to friction with water. By applying a hydrogel coating to the lower surface of the ship, existing large cargo ships can be much more fuel efficient.

As a result, my research in the Okano Laboratory has been to create a computer simulation to model the turbulent flow patterns at the surface of a ship. The virtual experimental apparatus is two concentric, counter-rotating cylinders with water between them. This flow is also known as Taylor-Couette Flow. As the inner cylinder rotates at a high velocity, the friction between the water and the cylinder surface resembles the underbelly of a ship sailing across water.

Direction numerical simulation (DNS, explicit method) and Large Eddy Simulation (LES, half approximation method) have been used to model the fluid flow. While DNS yielded solutions with 1.98% percentage error, LES models had 55% to 75% percentage error.

Future works include modifying the LES models to yield more accurate solutions with a lower computational cost. Once an LES control model has been achieved, we will simulate experiments with hydrogel coatings.

1. Introduction

Taylor-Couette (TC) flow has been of interest when G. I. Taylor mathematically and experimentally characterized its flow patterns in 1933 (Taylor 1933). The experimental apparatus explores the movement of fluid between two concentric, counter-rotating cylinders. The distinctive characteristic of TC flow is the formulation of Taylor Vortices (TV). At low Reynolds numbers, the flow is laminar couette flow. However, once the critical Reynolds number is reached, vortex pairs develop in the working fluid, transitioning the fluid flow into TC flow.

1.1 Terminology

The following notations will be used in this paper.

Ratio of the inner radius (r_i) to the outer radius (r_o):

$$\eta = \frac{r_i}{r_o}$$

The aspect ratio (Γ) is the ratio of the cylindrical length (L) to the length between the outer and inner radius:

$$\Gamma = \frac{L}{r_o - r_i}$$

Reynolds number (Re)

$$Re = \frac{r_i \Omega (r_o - r_i)}{\nu}$$

where r_i is the inner radius, r_o is the outer radius, Ω is the inner surface velocity, and ν is the kinematic viscosity.

Dimensionless Torque (G)

$$G \equiv \frac{T}{\rho \nu^2 L}$$

where T is torque, ρ is the density of water, ν is the kinematic viscosity of water, L is the height of the Taylor-Couette apparatus.

1.2 Turbulent Taylor-Couette Flow

The transition from laminar to turbulent in a TC apparatus is largely dependent on the Reynolds number, aspect ratio, and radius ratio. However, the exact criteria for turbulent transition are still unclear. For instance, Smith & Townsend (1982) report turbulence at Re=7300 (η=0.667), Andereck et al. (1986) report turbulent flow at Re=2890 (η=0.908), and Koschmieder (1979) at Re=1290 (η=0.727). Thus, there are no clear criteria for turbulent transition, but the start of the

transition is commonly agreed to start at Re=1000.

To better understand the underlying mechanisms of Taylor-Couette flow, scientists have replicated the flow using direct numerical simulations (DNS). Although numerical investigations have been carried out on TC flow, most of these experiments have been in the laminar regime due to computational costs. In contrast, most practical applications of TC flow, such as rotating machineries, viscosity measurements, rotating filters (Wereley 1999), and electrochemical processes (Gabe et al. 1998), operate in the turbulent regime. The major drawback in turbulent Taylor-Couette flow is its dissipative nature. Dissipative points occur throughout the turbulent fluid and lead large computation costs. As a result, turbulent Taylor-Couette flow has not been extensively explored through numerical simulations.

At high Reynolds numbers, Direct Numerical Simulation (DNS) requires extremely fine meshes, which also results in high computational cost. As an alternative, Reynolds-Averaged Navier Stokes (RANS) and Large Eddy Simulation (LES) are preferred. RANS is a time-average solution, which greatly reduces the computational cost associated with the fluctuating quality of turbulence flow. While RANS approximates the whole system, LES models the system by explicitly solving the large eddies and approximating small scale solutions using a filter.

For my experiment, I modeled Taylor-Couette Flow at Re=5000 using DNS, One Equation Eddy (oneEqEddy, LES), and Smagorinsky (LES).

Due to the nature of the flow, its acute measurements of the flow often do not get the full picture. Using numerical simulations, laminar Taylor-Couette flow has been better understood. However, the major problem still lies in numerically simulating turbulent Taylor-Couette flow.

1.3 Objective
1.11
Explore the relationship of DNS computational cost with increase in Reynolds number.

The objective of this experiment is to develop a working Taylor-couette turbulent model for hydrogel surface coating tests. Currently, Okano et al is working on drag reduction effect using hydrogel coating to reduce energy loss on large transport cargo ships. The purpose of my numerical simulation

is to create a model that replicates our experimental results to better understand the microscopic differences with and without the presence of hydrogels.

To reduce for computational costs, Reynolds-Averaged Navier-Stokes (RANS) and Large Eddy Simulation (LES) models are often applied. The objective of my experiment is to create three working models: DNS, one Equation Eddy, and Smagorinksy.

2. Methods

2.1 Experimental Set Up

The first step of my research was to create a working model of the experimental apparatus that we have in the laboratory.   The dimensions of my Taylor-Couette model had an inner radius of 48mm, outer radius of 64mm, and height of 122.5mm (η=0.75, Γ=7.66).   Our numerical grid was classified as the following:

Grid Class	Radial Split	Theta Split	Height Split	Total Number of Cells
Coarse	32	144	96	442,368
Fine	56	256	172	2,465,792

Simple grading was applied to the grid to yield more precise measurements in the dynamic regions of the calculation. The grid at the inner rotating wall is four times finer than the grid used near the stationary outer wall.   Additionally, the grid at the top and bottom of the cylinder is also eight times finer than the grid used in the middle of the cylinder.

The following governing equations were assumed for the incompressible and Newtonian fluid.

<div align="center">Continuity</div>

$$\nabla \cdot \boldsymbol{u} = 0$$

<div align="center">Navier-Stokes Equation</div>

$$\frac{\partial \boldsymbol{u}}{\partial t} + \boldsymbol{u} \cdot \nabla \boldsymbol{u} = -\frac{\nabla \boldsymbol{P}}{\rho} + \nu \nabla^2 \boldsymbol{u}$$

where $\boldsymbol{u}$ is the velocity of the fluid, $\boldsymbol{P}$ the pressure, ρ the fluid density, and ν the kinematic density.

2.2 Low Reynolds Number and Computational Cost

The first experiment was to correlate Reynolds number with computational cost. Using lab5-2's processing hardware (Intel Xeon W5580 3.2GHz, 24GB memory), Taylor-Couette flow simulation were performed at Re=500, Re=1000, and Re=2000 using coarse mesh grading with Courant Number=0.1.

2.3 Re=5000 and Computational Methods

First, I reached steady-state in my Taylor-Couette system by executing oneEqEddy model with coarse mesh from time 0 seconds to time 200 seconds, using 16 parallel super computers cores from Kyoto University. The Courant Number was chosen to be 0.2. After reaching 200seconds, I created three new experiments with the numerical schemes of DNS, oneEqEddy, and Smagorinsky using fine meshes. The mapFields command was used in OpenFOAM to convert from coarse mesh to fine

mesh.   The decomposition method for all core splitting actions were scotch.

2.3.1 Direct Numerical Simulation (DNS)

The DNS calculation modeled the flow as laminar in turbulenceProperties using fine mesh with simple grading.

2.3.2 One Equation Eddy (oneEqEddy)

OneEqEddy model was selected by choosing LESModel in turbulenceProperties, oneEqEddy in LESProperties, and cubeRootVol for delta.   The cubeRootVol delta coefficient was chosen as default 1.   NuSgs in the initial condition folder was set to nuSgsUSpaldingWallFunction with uniform 0.0000001 value for all four walls (top, bottom, inner, outer).   The simulation was performed two times using fine mesh with simple grading and fine mesh with uniform grading. The code below was oneEqEddy model criteria in oneEqEddy.H from OpenFOAM.

```
One Equation Eddy Viscosity Model for incompressible flows

    Eddy viscosity SGS model using a modeled balance equation to simulate the
    behaviour of k, hence,

        d/dt(k) + div(U*k) - div(nuEff*grad(k))

        =

        -B*L - ce*k^3/2/delta
    and
        B = 2/3*k*I - 2*nuSgs*dev(D)
        Beff = 2/3*k*I - 2*nuEff*dev(D)
    where
        D = symm(grad(U));
        nuSgs = ck*sqrt(k)*delta
        nuEff = nuSgs + nu
```

2.3.3 Smagorinsky

Smagorinsky model was selected by choosing LESModel in turbulenceProperties, Smagorinsky in LESProperties, and cubeRootVol for delta. The cubeRootVol delta coefficient was chosen as default 1. NuSgs in the initial condition folder was set to nuSgsUSpaldingWallFunction with uniform 0.0000001 value for all four walls (top, bottom, inner, outer). The simulation was performed two times using fine mesh with simple grading and fine mesh with uniform grading. The code below was the Smagorinsky model criteria in Smagorinsky.H from OpenFOAM.

```
The Isochoric Smagorinsky Model for incompressible flows.

    Algebraic eddy viscosity SGS model founded on the assumption that

    local equilibrium prevails.

    Thus,

        B = 2/3*k*I - 2*nuSgs*dev(D)

        Beff = 2/3*k*I - 2*nuEff*dev(D)

    where

        D = symm(grad(U));

        k = (2*ck/ce)*delta^2*||D||^2

        nuSgs = ck*sqrt(k)*delta

        nuEff = nuSgs + nu
```

3. Results

3.2 Low Reynolds Number and Computational Cost
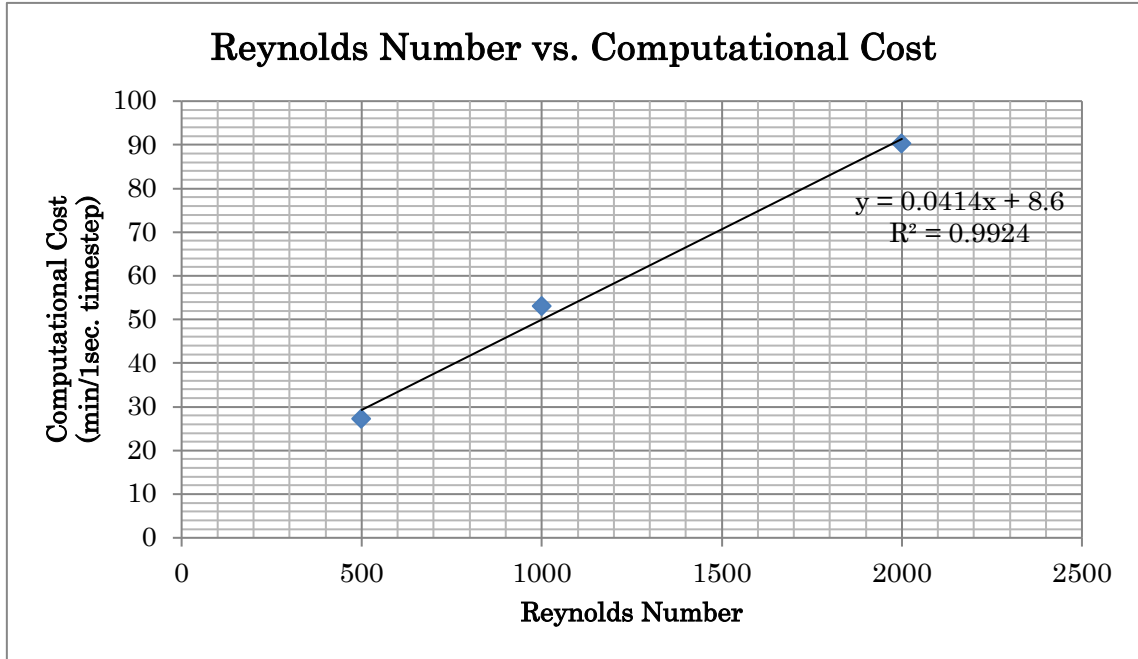
Figure 1: Relationship between Reynolds Number and Computational Cost

Figure 1 shows the relationship between Reynolds number and computational for Intel Xeon W5580 3.2GHz, 24GB memory when processing a Taylor-Couette experiment with coarse mesh. The relationship seem to be linear with an equation of y=0.0414x+8.6 and an R^2 value of 0.9924.

3.3 Re=5000 and Computational Methods

Figure 3 shows the simple grading numerical fine grid mesh used in the experiment. Fig. 3(a) shows the grid as a whole, Fig. 3(b) a vertical slice of the grid, and Fig. 3(c) a horizontal view of the grid. The diagonal cut pattern in Fig. 3(b) was the result of slicing the cylinder for visualization.
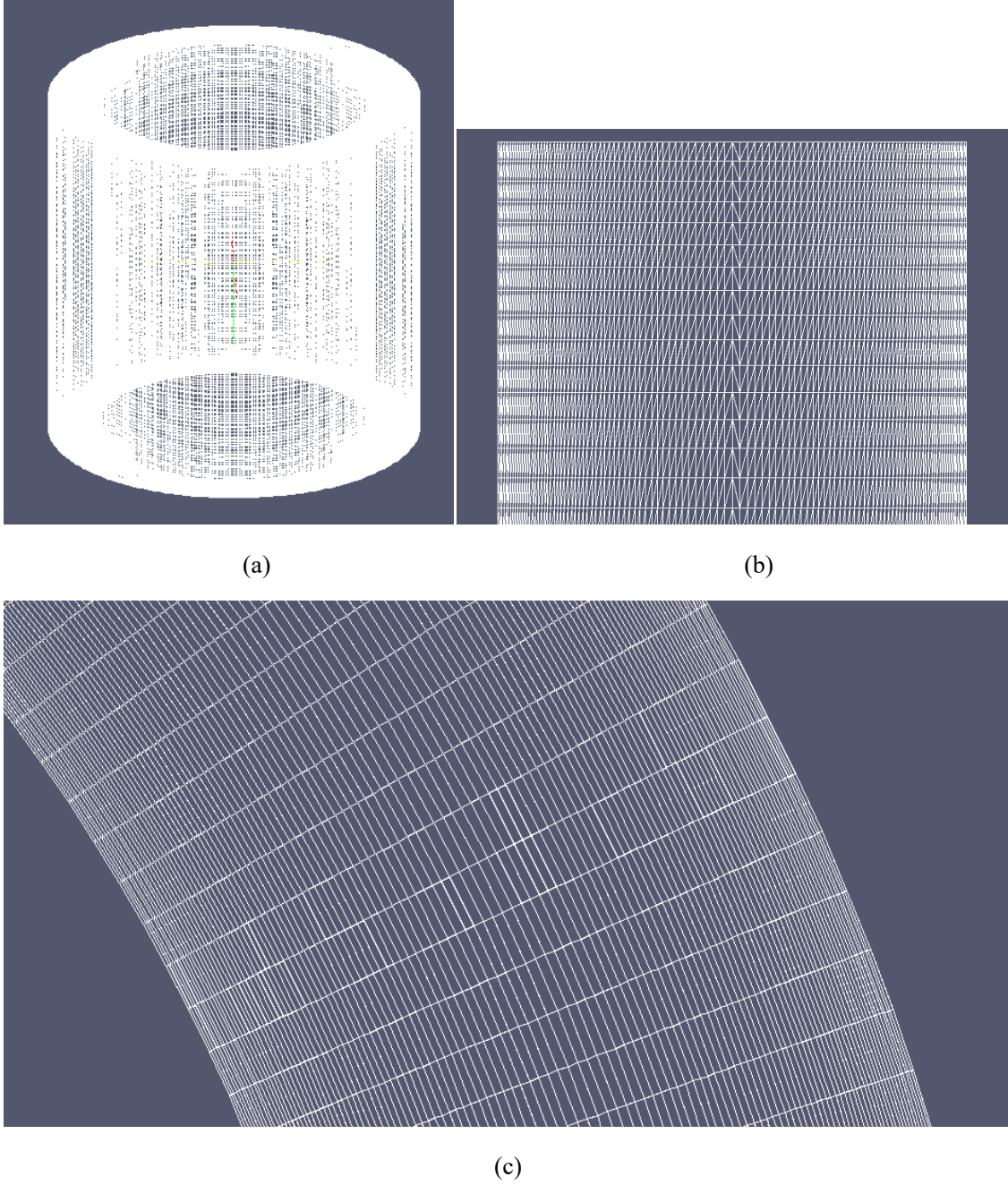
(a)

(b)

(c)

Figure 3: visualization of the simple grading fine mesh grid

The computational costs per 1 second time step were analyzed from all simulations in Table 1. 36 cores were provided by Kyoto University; thus, only a limited number of simulations can be executed simultaneously. Eight cores were allocated to each simple grading experiment at the 200 second mark. 16 cores were allocated to each uniform grading experiment for comparison with the simple grading experiments.

Method	Grading Type	Number of Cores	Start Time (sec)	End Time (sec)	Computational Cost per 1sec Time Step (min/sec)
OneEqEddy	Simple	16	0	200	14.7
DNS	Simple	8	200	276.8	131.3
OneEqEddy	Simple	8	200	263.2	125.5
Smagorinsky	Simple	8	200	226.7	297.6
OneEqEddy	Uniform	16	200	303.6	97.3
Smagorinsky	Uniform	16	200	310.2	91.5

Table 1: List of simulations and their computational cost

Table 1 was recreated into column graphs for better comparison between similar test cases in Figure 3.

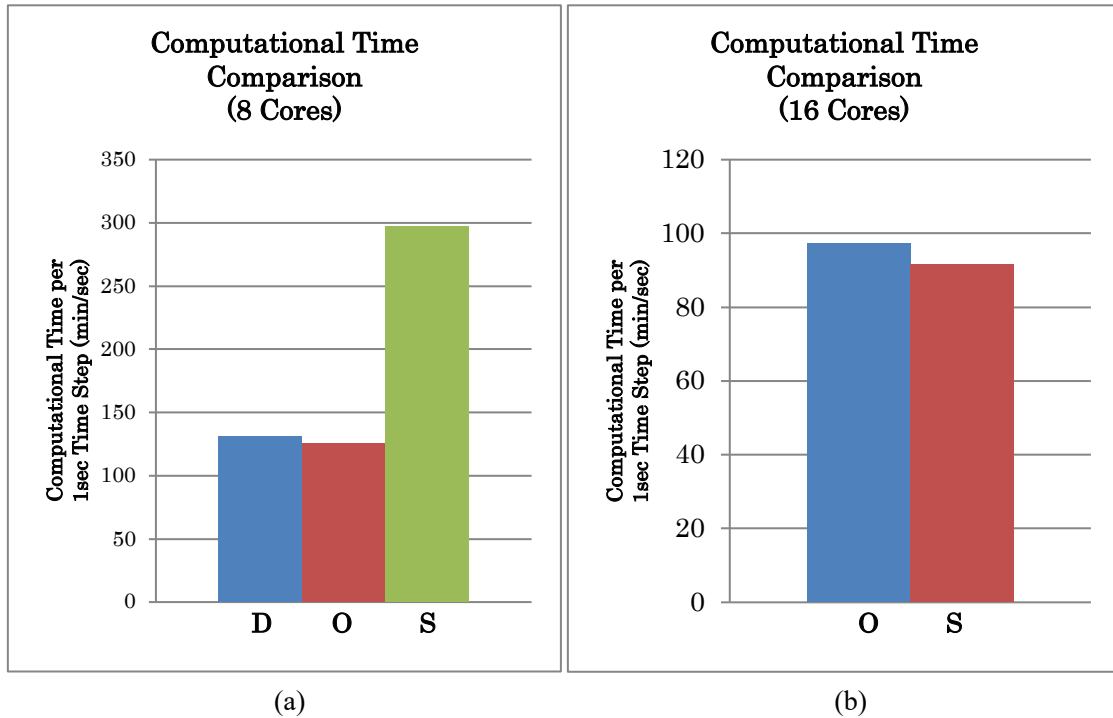(a)   (b)

Figure 3: Computational time comparison between cases performed on Kyoto's super computers. In the charts, DNS is abbreviated as D, One Equation Eddy as O, and Smagorinsky as S.

Figure 4(a) shows the non-dimensional torque (G) as each numerical scheme reached steady-state after 200 seconds. The torque values for each steady-state system were averaged between 205 seconds and 210 seconds.   The fluctuations of G between this time period is enlarged in Fig. 4(b), and the averaged values are displayed in Table 2. **Note: The graphs made in Figure 4 are not complete.   Microsoft had problems displaying all data points from the experiment.**
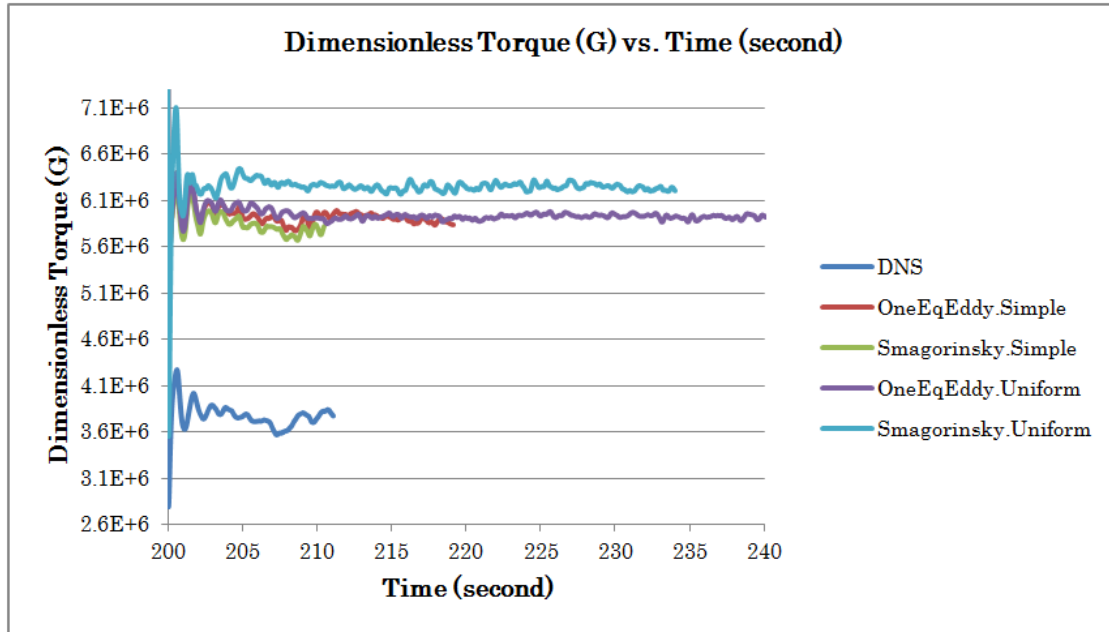
(a)
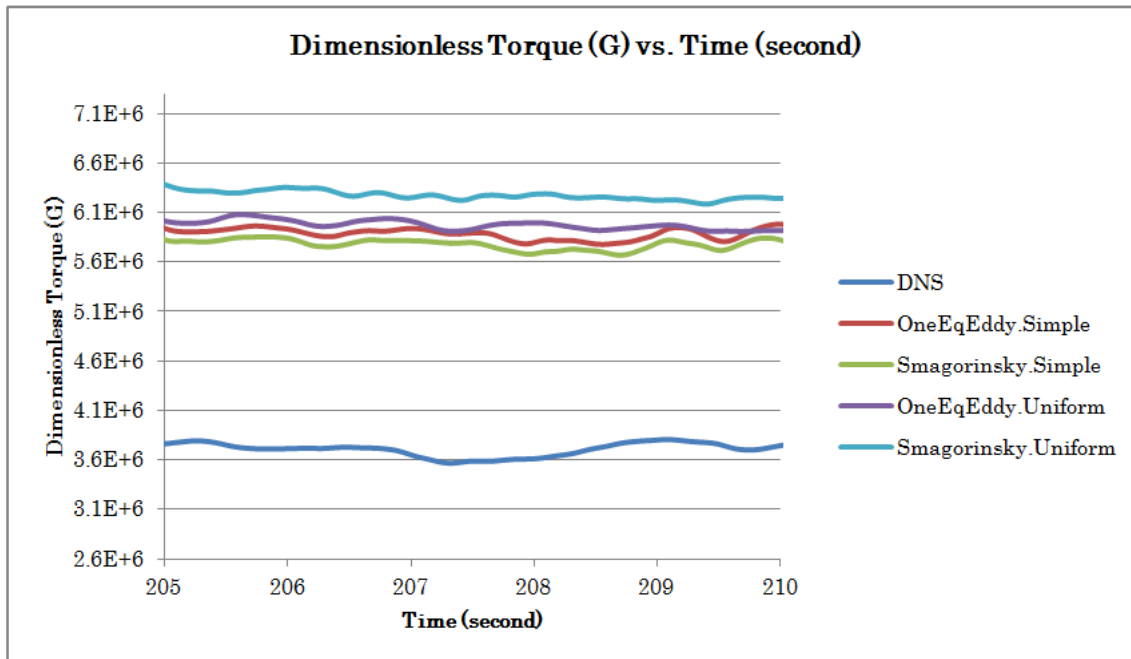
(b)

Figure 4: the relationship between dimensionless torque (G) and time for the turbulent experiments after 200 seconds; (b) is an enlargement of the time period 205 to 210 seconds of (a).

Method	Grading Type	Dimensionless Torque (G)
DNS	Simple	3,709,271.262
OneEqEddy	Simple	5,889,796.963
Smagorinsky	Simple	5,776,083.388
OneEqEddy	Uniform	5,972,277.079
Smagorinsky	Uniform	6,289,012.261

Table 2: the dimensionless torque values for each turbulent experiment, averaged between 205 and 210 seconds.

The non-dimensional distance for Smagorinsky and OneEqEddy, simple and uniform experiments are displayed in Figure 5.
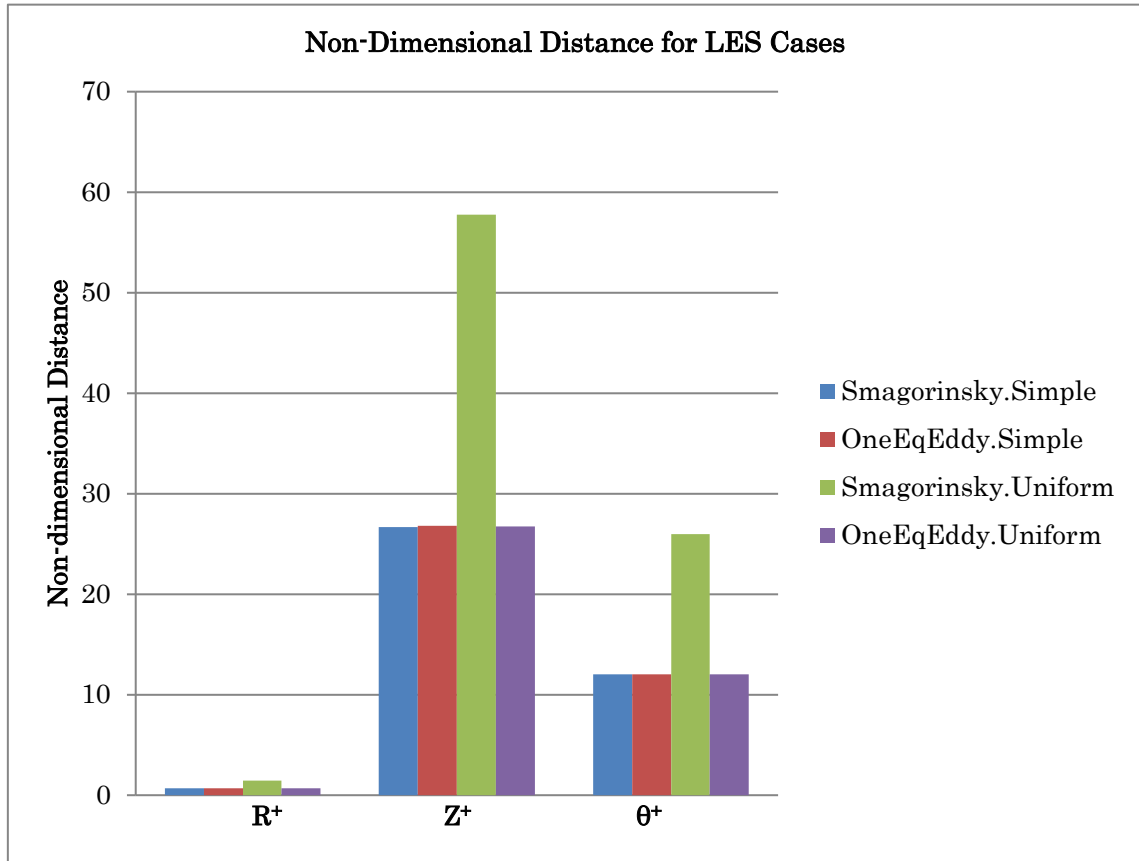

Figure 5: Non-dimensional distance for the LES cases.

The Q-criterion was used to visualize turbulence on the LES cases.   Figure 6 shows the contour of the LES cases when Q = 80.
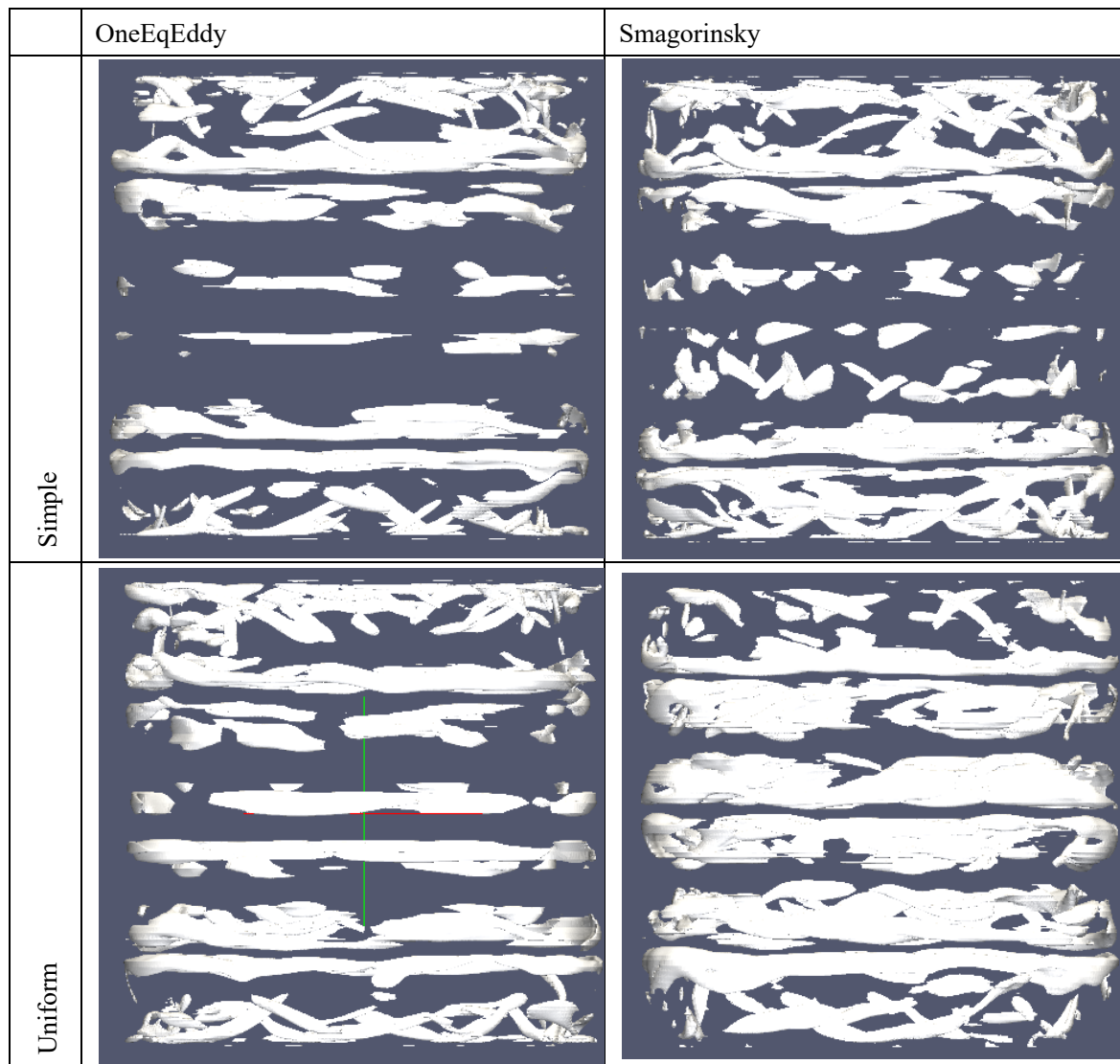
	OneEqEddy	Smagorinsky
Simple		
Uniform		

Figure 6: Q-criterion = 80 visualization for One Equation Eddy and Smagorinsky in simple and uniform grid cases.

4. Discussion

Using empirical methods F. Wendt proposed the following relationship between dimensionless torque per unit length (G) and Reynolds number (1933).

$$G = 1.45 \frac{\eta^{3/2}}{(1 - \eta)^{7/4}} Re^{1.5} \quad , \quad 400 < Re < 10^4$$

Wendt's empirical solution was used to test the accuracy of our quantitative results. In Figure 7, the dimensionless torque from Wendt's solution is compared with our numerical results.   The percentage error from Wendt's empirical solution is displayed in Table 3 from lowest to highest along with each simulation's computational cost per 1second of time step.
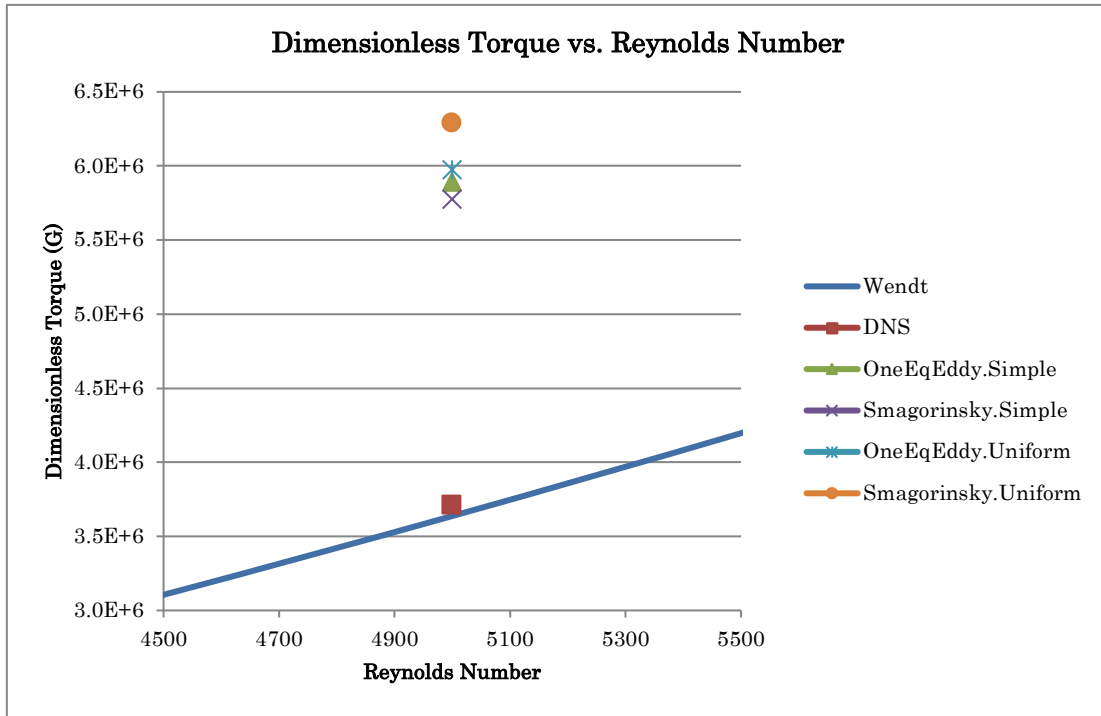

Figure 7: Comparison of numerical results with Wendt's empirical solution

	DNS	Smagorinsky Simple	OneEqEddy Simple	OneEqEddy Uniform	Smagorinsky Uniform
Torque Percentage Error	1.98%	58.80%	61.93%	64.20%	72.90%
Computational Cost per 1sec Time Step (min/sec)	131.3	297.6	125.5	97.3*	91.5*

*Table 3: the non-dimensional torque (G) percentage error with associated computational cost per 1sec time step for each simulation after 200 seconds. *The uniform grid experiments were performed with 16 cores; whereas, other experiments were performed with 8 cores.*

From Table 3, the accuracy of each experiment can be quantified. Direct numerical simulation

(DNS) had the highest accuracy with 1.98% deviation from Wendt's empirical solution. The Large Eddy Simulations (LES) all have similar error margin between 55% to 75% deviation from Wendt's empirical solution. Within the LES experiments, the accuracy with simple grading grid is higher than experiments with uniform grid.

The main reason for using LES is to reduce computational cost while maintaining an accurate solution. However, my LES models were extremely inaccurate when compared to the DNS solution and the computational cost was not greatly reduced. I believe the main cause is the filter criteria, which is the delta function. In my experiments, all LES models used cubeRootVol at default ratio of 1 for approximation. The cubeRootVol delta function sets the size of approximation to be the cube root of volume of each cell. Reducing the ratio should reduce the error margin.

Furthermore, the non-dimensional distance for LES cases (see Figure 5) show an uneven distribution in the r, θ, and z direction. Although r^+ was justly low because velocity varies the most in the r-direction, I believe that θ^+ and z^+ are too high for accurate approximation in LES. Even though the large spacing in θ and z produced an accurate DNS approximation, I believe that this large spacing in the θ and z direction may have led to poor approximations in LES.

There may be a correlation between the non-dimensional distance and accuracy of the model. When comparing the error of experiments (Table 3) with its non-dimensional distance (Figure 5), Smagorinsky with uniform spacing yield high in both categories. However, this relationship does not hold for OneEqEddy.Simple and OneEqEddy.Uniform experiments. One Equation Eddy with uniform spacing had smaller non-dimensional distances for r, θ, and z, but still yielded a higher percentage error.

The computational cost for Smagorinsky with simple grading was unexpectedly high for an LES model when compared to the OneEqEddy model with simple grading (see Table 3). In the following experiment using uniform grid and 16 cores, Smagorinsky performed more efficiently than OneEqEddy model. The exact reason for the high computation cost with Smagorinsky using simple grading is unclear.

Taylor, G. I. 1923 Stability of a viscous fluid contained between two rotating cylinders. Phil. Trans. R. Soc. Lond. **223**, 289–343.

Gabe, D. R., Wilcox, G. D., Gonzales-Garcia, J. & Walsh, F. C. 1998 The rotating cylindrical electrode: its continued development and application. J. Appl. Electrochem. **28**, 759–780.

Wereley ST, Lueptow RM. 1999. Inertial particle motion in a Taylor-Couette rotating filter. Phys Fluids 11:325–333.

Smith, G. P. & Townsend, A. A. 1982 Turbulent Couette flow between concentric cylinders at large Taylor numbers. J. Fluid Mech. **123**, 187–217.

Andereck, C. D., Liu, S. S. & Swinney, H. L. 1986 Flow regimes in a circular Couette system with independently rotating cylinders. J. Fluid Mech. **164**, 155–183.

Koschmieder, E. L. 1979 Wavelength measurements in turbulent Taylor vortex flow. J. Fluid Mech. **93**, 515–527.